Characterization of elastic parameters of point and line excited porous materials by means of the wave correlation method, Hankel functions and Mindlin's plate theory; a numerical study.

N.B. Roozen
KU Leuven, Laboratory of Acoustics, Department of Physics, Celestijnenlaan 200D, Leuven, Belgium.
NOVIC Noise and Vibration Control, Burg.Strijbosstraat 1, 5591EL Heeze, the Netherlands

Paolo Bonfiglio
Materiacustica srl - Via C. Ravera 15 A 44122 Ferrara, Italy.

Francesco Pompoli
Department of Engineering, University of Ferrara, Via Saragat 1, 44122 Ferrara, Italy.

Summary

This paper reports on the characterization of the mechanical properties of a point excited and line excited porous material by means of the inhomogeneous wave correlation approach based on the Hankel's function. The correlation approach allows the wavenumber to be complex. Both propagating waves and evanescent waves are considered. Excitation along a line is approximated by means of an array of points. First order reflections from the edges are taken into account by mirror images. The material properties, in terms of Young's modulus and loss factor, are estimated by means of Mindlin's plate theory. The obtained results are compared with Kirchhoff's thin shell theory and Lamb wave theory.

A numerical model was used to simulate measurements on a porous sample. Knowing the material properties a priori (i.e. the properties that were used as input to the numerical simulation), opened the possibility to check the correctness of the characterization procedure and zoom in on possible deviations.

It was found that at higher frequencies and thicker slabs Kirchhoff's thin shell theory is clearly insufficient. It was also found that for the frequency range and thicknesses studied, Mindlin's plate theory and Lamb wave theory are not very much different (error in wavenumber less than 2% for frequencies up to 1000 Hz and thicknesses up to 10 mm). Good results were obtained for the Young's modulus and the loss factor of the slab material by considering evanescent waves and reflections from the edges of the slab by means of mirror images, using Mindlin's thick plate theory. Taking into account the first order reflection seems sufficient for the type of slab and frequencies considered.

PACS no. 43.20.Jr

1. Introduction

Characterisation of porous material can be done in several manners, the most commonly used approach being a compression test. Less common, is a Lamb wave experimental test, in which a shaker excites the slab at one point and a scanning Laser Doppler Vibrometer (LDV) probes the vibrational response at a number of positions (see Figure 1). Thus the vibrational response is measured as function of frequency and position, allowing to assess the dispersion relationships of the material, and from that, the material properties.

This paper focusses on the Lamb wave experimental test. A numerical (FEM) model is used to generate the 'measurement' data. Material characterization is attempted in a number of ways.

2. Materials and methods

The sample studied is a porous material with the dimensions and material properties as mentioned in Table I. The material is assumed to be homogeneous,

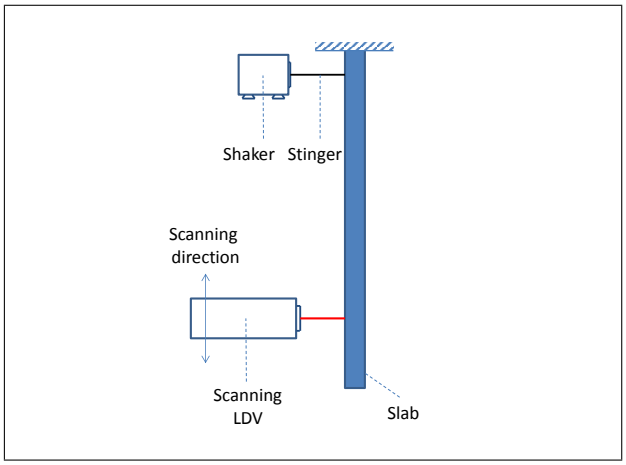

Figure 1. Lamb wave experimental set-up, with shaker and scanning Laser Doppler Vibrometer (LDV)

Table I. Dimensions and material properties porous material studied.

Young's modulus	3.5e5 $(1 + 0.3 \cdot \mathrm{i})$ Pa
Poisson's ratio	0.33
Density	48 kg/m^3
thickness	2.5 mm and 10 mm
width	50 cm
height	50 cm

made from a solid material with mentioned material properties. Two configurations were studied. In configuration 1 (Figure 2) the sample was point excited at the top, having symmetry boundary conditions acting on this edge. In configuration 2 (Figure 3) the sample was clamped at the top, and excited by means of a shaker along a line. In practice, this can be done by mounting a knife to the shaker. This line was positioned 3.5 cm below the clamped edge, and has a length of 10 cm. Simulations were performed by means of the finite element method.

The resulting responses were computed along a line of points located on the line of symmetry (indicated by a dash-dotted line in Figures 2 and 3) for a range of frequencies. The characterization of the material was performed by fitting these responses by means of a wave correlation procedure, involving complex valued propagating waves and evanescent waves. This approach is briefly described in the next subsections.

2.1. Theory of the wave correlation method for a point excited, finite samples

2.1.1. Kirchhoff's thin plate theory

The theory that is used in this paper is described by Roozen et. al [1]. In this section a brief summary is given.

Basically, the approach in [1] fits vibrational (measurement) data by means of the fundamental solution (the Green's function) of a thin, point-excited, infinite plate. This Green's function corresponds to a Hankel

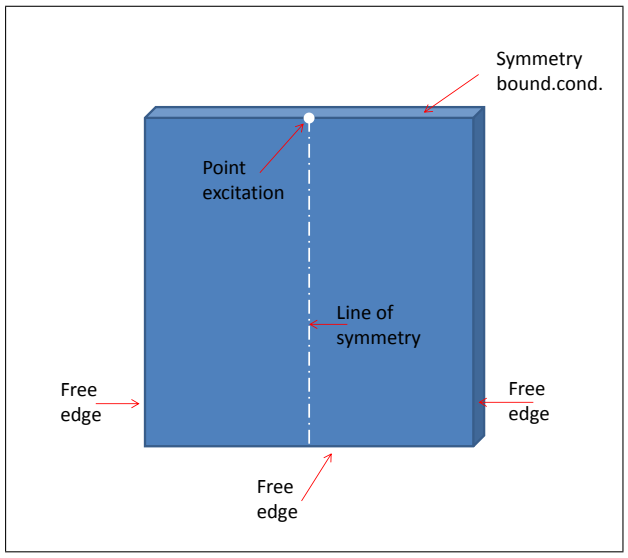

Figure 2. dimensions and boundary conditions of simulated foam slab, point excitation.

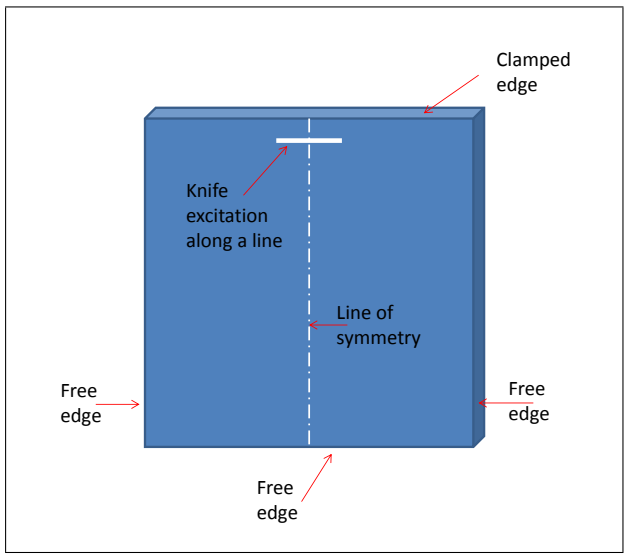

Figure 3. dimensions and boundary conditions of simulated foam slab, knife excitation.

function, and reads

$$\Phi\left(x, y, x_0, y_0\right) = \frac{1}{8k_f^2 D}\left(H_0^{(1)}\left(k_f\|r\|\right) - H_0^{(1)}\left(ik_f\|r\|\right)\right) \quad (1)$$

where $H_0^{(1)}$ is the cylindrical Hankel's function of the first kind of order 0, and $\|r\| = \|(x - x_0, y - y_0)\|$ is the source-to-receiver distance.

The vibrational (measurement) data w is fitted by searching for an optimal projection of the vibrational data on to a number of Green's function Φ, contained in a matrix $\mathbf{\Phi}$, each Green's function either representing the waves emanating from the point of excitation, or from reflections from the boundaries using an image source approach (see [1] for more details). For this

purpose the projected vibrational field $\tilde{w}$ is computed with

$$\tilde{w} = \mathbf{\Phi}\mathbf{\Phi}^{+\lambda} w. \tag{2}$$

where '$+\lambda$' represents the generalized inverse (possibly regularized with parameter λ; see [1]). The adequacy between matrix Φ and measurements w is quantified by the following normalized reconstruction error

$$e = \frac{\|w - \tilde{w}\|^2}{\|w\|^2}, \tag{3}$$

Minimizing this error e by varying the complex wavenumber k_f in Eq. 1, yields an important stiffness- and damping parameter that characterizes the material.

Using Kirchhoff's theory of thin plates, the dynamic flexural rigidity $D_{Kirchhoff} = {E_{Kirchhoff} h^3}/{12\,(1-\nu^2)}$ and the flexural wave number k_f are related by the equation

$$k_f = \left(\omega^2 \frac{\rho h}{D_{Kirchhoff}}\right)^{1/4} \tag{4}$$

where h is the plate thickness Thus the Young's modulus $E_{Kirchhoff}$ can be determined from the fitted wavenumber k_f, assuming some value for the Poisson's ratio ν (usually taken to be 0.3).

In the above it is assumed that Kirchhoff's theory of thin shells can be used.

2.1.2. Mindlin's thick plate theory

When dealing with thick plates other theories should be employed. Lamb wave theory is an 'exact' theory for thick plates. The computation, however, is a bit cumbersome, requiring an implicit iteration in a search for vanishing determinants. A good compromise, which allows an explicit expression of Young's modulus, is Mindlin's theory of thick plates. Following Rose et al. [2] (Eq. 52b) the deflection of a thick plate due to a point excitation (i.e. the Green's function) is given by

$$\Phi\left(x, y, x_0, y_0\right) = \frac{1}{4D}\left(\frac{H_0^{(1)}\left(k_1 r\right)}{\left(k_1^2 - k_2^2\right)\gamma_1} - \frac{H_0^{(1)}\left(k_2 r\right)}{\left(k_1^2 - k_2^2\right)\gamma_1}\right) \tag{5}$$

where D is the dynamic stiffness, k_1 and k_2 are the pertinent roots (wavenumbers) representing either traveling or evanescent waves, respectively (in the latter case, k_2 is an imaginary number), and γ_1 is some (frequency and wavenumber dependent) scaling factor. Thus for the purpose of this paper it is sufficient to consider the following two fundamental functions for the computation of the optimal projection by means of Eq. 2, contained in a matrix $\mathbf{\Phi}$:

$$\mathbf{\Phi} = \left[H_0^{(1)}\left(k_1 r\right) \quad H_0^{(1)}\left(k_2 r\right)\right] \tag{6}$$

where k_1 is a real-valued wavenumber (the propagating part) and k_2 is an imaginary-valued wavenumber (the evanescent part).

Actually, when comparing this result with the Green's function that were given in the previous section, Eq. 1, we see that the test functions contained in $\mathbf{\Phi}$ are the same. There is only one subtle difference, in that in Eq. 1 the evanescent wavenumber is the same in magnitude as the propagating wavenumber, whereas in Eq. 5 they can (and generally will be) different (k_1 and k_2). In the following section, the evanescent and propagating wavenumbers are allowed to be different in magnitude.

If needed, the matrix $\mathbf{\Phi}$ can be extended by a couple of propagating and evanescent waves emanating from reflecting boundaries using an image source approach (see [1] for more details). Next, the optimal wavenumber pair (propagating and evanescent) can be searched for using Equation Eq. 2 and minimizing Eq. 3.

The complex valued Young's modulus $E_{Mindlin}$ can be estimated from the fitted value for k_1 using the formula [3]

$$E_{Mindlin} = (A \pm B)\rho(1-\nu^2)v_{fit}^2/2 \tag{7}$$

with

$$v_{fit} = {\omega}/{k_1} \tag{8}$$

$$\kappa = {(0.87 + 1.12\nu)}/{(1+\nu)} \tag{9}$$

$$A = 1 + {2(1+\nu)}/{\kappa(1-\nu^2)} + {12 v_{fit}^2}/{d^2\omega^2} \tag{10}$$

$$B = \sqrt{A^2 - {8(1+\nu)}/{\kappa(1-\nu^2)}} \tag{11}$$

where ν is Poisson's ratio, ω is the radian frequency, and d is the thickness of the plate.

2.2. Dealing with excitation along a line (knife excitation)

Knife excitation is sometimes used with the idea to generate plane waves. Although this can only be achieved within a limited number of wavelengths from the source, it is often being done by experimental physicists.

A line excitation (configuration 2; see Figure 3) can be approximated by a sum of point sources, located on this line and acting 'in phase'. Thus the Green's function Φ, in case of Kirchhoff's thin shell theory, is constructed as follows

$$\mathbf{\Phi} = \left[\sum_{i=1}^{N} H_0^{(1)}\left(k_1\sqrt{(x_i^2 + y^2)}\right) \quad \sum_{i=1}^{N} H_0^{(1)}\left(k_2\sqrt{(x_i^2 + y^2)}\right)\right] \tag{12}$$

where the line excitation is represented by N discrete points with coordinates x_i, i=1...N and y is the distance from the point of excitation on the line of symmetry.

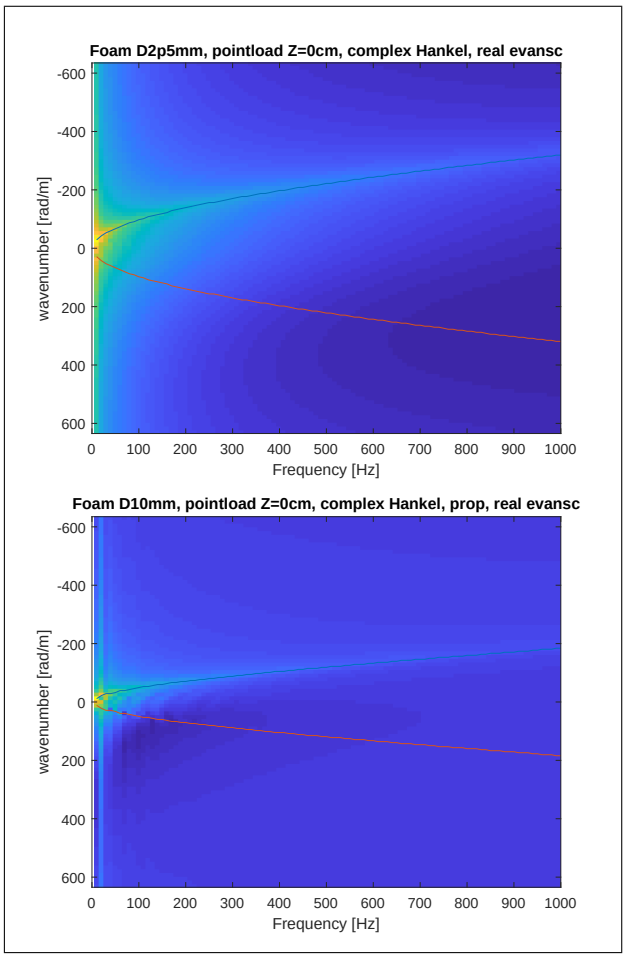

Figure 4. $k-\omega$ spectrum of point excited slap (Figure 2), 2.5mm thick (top) and 10mm thick (bottom). Color image $k-\omega$ spectrum obtained by measn of classical spatial Fourier transform. Solid lines obtained by means of complex wavenumber fit including propagating and evenescent waves (real part of k shown only).

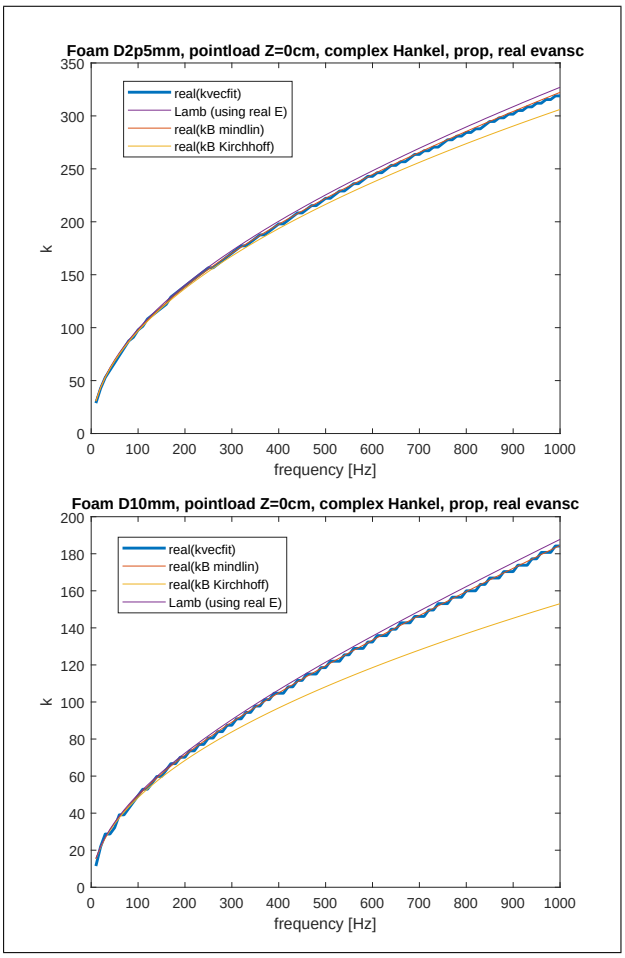

Figure 5. Real part of the wavenumber as function of frequency, for a point excitated slap (Figure 2), 2.5mm thick (top) and 10 mm thick (bottom). Thick blue cure shows the fit result based on Mindlin's theory. Thin curves give the real part of the wavenumber according to Lamb theory, Mindlin theory and Kirchoff theory for the nominal material properties.

3. Fit results

As the 'measurement' data was created numerically by means of a finite element model, the material properties are known a priori (see Table I). The material properties are obtained by fitting the vibrational 'measurement' data using Mindlin's theory as described in Section 2.1.2. The vibrational 'measurement' data were computed for a number of points located on the line of symmetry (indicated by a dash-dotted line in Figures 2 and 3)

Figure 4 shows a color image of the $k-\omega$ spectrum of the point excited slap (Figure 2), 2.5mm thick and 10mm thick, as obtained from the 'measurement' data by means of a classical spatial (1D) Fourier transform. The real part of the fitted wavenumber, using the theory given in Section 2.1.2, is shown in this figure as a solid curve as well.

Figure 5 shows the real part of the fitted (propagating) wavenumber as function of frequency. The thick cure shows the fit result based on Mindlin's theory, searching in complex propagating wavenumber domains and real evanescent wavenumber domain (thus in 3 dimensions). The thin curves give the real part of the wavenumber as function of frequency according to Lamb theory, Mindlin theory and Kirchoff theory, for a slab with the (a prior known) nominal material properties as mentioned in Table I. It is clear that the fit procedure gives wavenumber results that follows the nominal curve for Mindlin's theory. From the figure it can also be seen that Lamb theory and Mindlin's theory are relatively close to each other, with deviations of less than 2% up to 1000 Hz (thickness slab 10 mm; see bottom graph in Figure 5). Kirchhoff's theory gives largely different results, especially for thick slabs and higher frequencies. Clearly Kirchhoff's thin shell theory is not adequate for the slabs and frequency range that were studied in this paper.

Figure 6 shows the Young's modulus and the loss factor according to Mindlin's theory (i.e. using the complex valued wavenumber fit results and Eq. 7) for

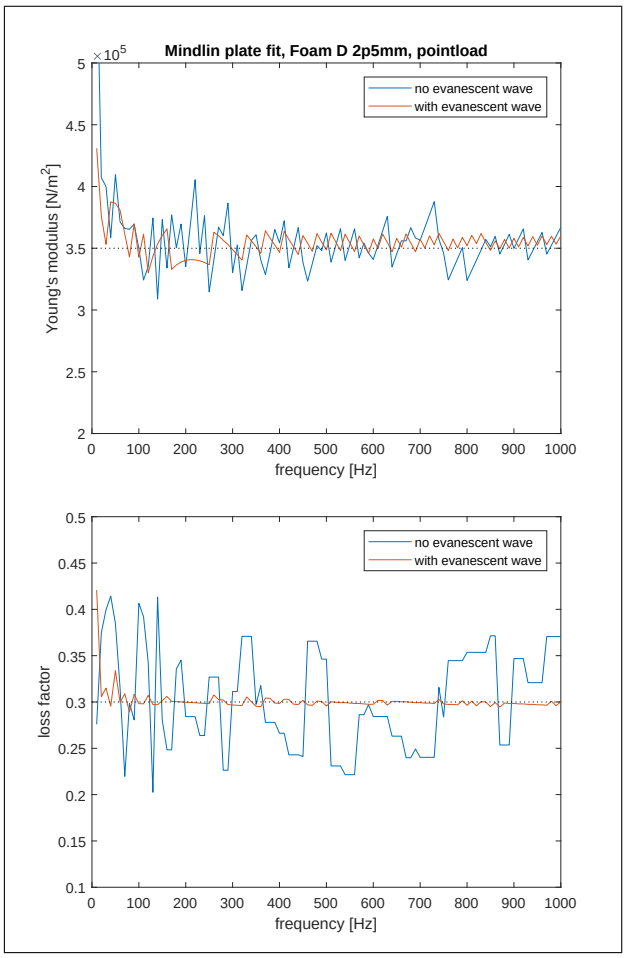

Figure 6. Point excitated slap (Figure 2), 2.5mm thick, Young's modulus (top) and loss factor estimate (bottom) based on Mindlin's theory. Blue curve: complex Hankel fit without evenscent wave component, Red curve: complex Hankel fit with evenscent wave component.

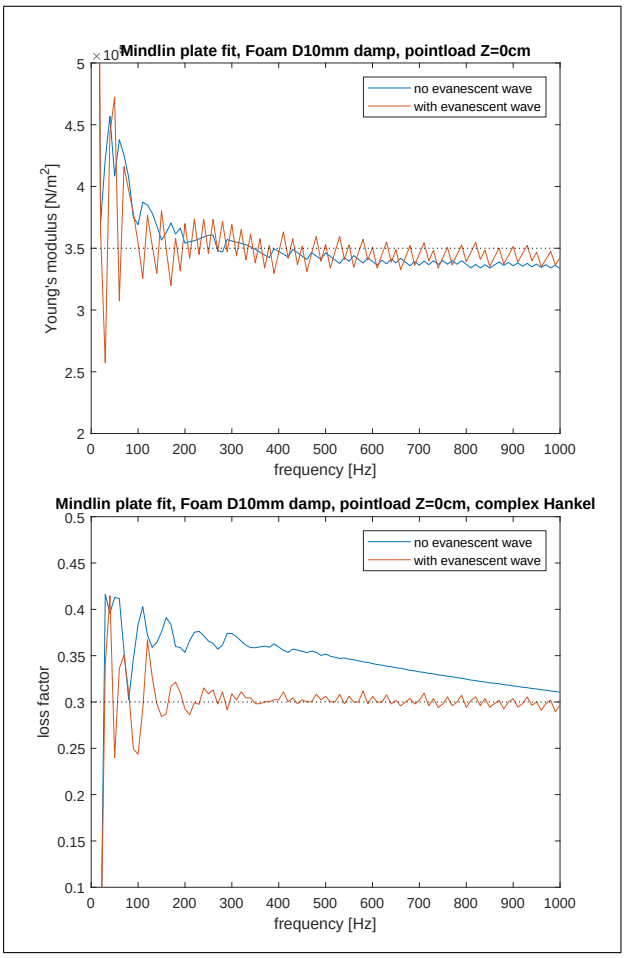

Figure 7. Point excitated slap (Figure 2), 10mm thick, Young's modulus (top) and loss factor estimate (bottom) based on Mindlin's theory. Blue curve: complex Hankel fit without evenscent wave component, Red curve: complex Hankel fit with evenscent wave component.

a slab of 2.5 mm thickness. The loss factor is computed as the ratio of the imaginary part of the Young's modulus over the real part of the Young's modulus. In this figure the resulting Young's modulus and loss factor are also shown in case the evenescant waves are not considered. From this figure it can be concluded that the inclusion of evanescent wavenumbers for the computation of the projected vibrational field (Eq. 2) and to minimize the projection error e (Eq. 3) is important in order to obtain a certain degree of accuracy.

Figure 7 shows the Young's modulus and the loss factor according to Mindlin's theory (i.e. using the complex valued wavenumber fit results and Eq. 7) for a slab of 10 mm thickness, point excited at the top edge. The conclusions are similar: evanescent waves should be included in the search for an optimal projection of the 'measurement' data.

Figure 8 shows a color image of the $k-\omega$ spectrum of the line excited slap (Figure 2), 10mm thick, as obtained from the 'measurement' data by means of a classical spatial (1D) Fourier transform. The real part of the fitted wavenumber, using the theory given in Section 2.1.2, is shown in this figure as a solid curve as well. Again, a complex valued propagating wavenumber was searched for, as well as a (real valued) evanescent wavenumber (thus searching in 3 dimensions), to minimize the error e in Eq. 3.

Figure 9 shows the Young's modulus and the loss factor according to Mindlin's theory (i.e. using the complex valued wavenumber fit results and Eq. 7) for a line-excited slab of 10 mm thickness. The figure shows fit results in which the first-order reflection from the top edge is taken into account, for both the propagating (complex) waves and the evanescent waves. Not taking into account the reflection and / or the evanescent waves reduces the accuracy of the fit results.

4. CONCLUSIONS

Using numerically computed vibrational responses of a slab of porous material with various thicknesses the

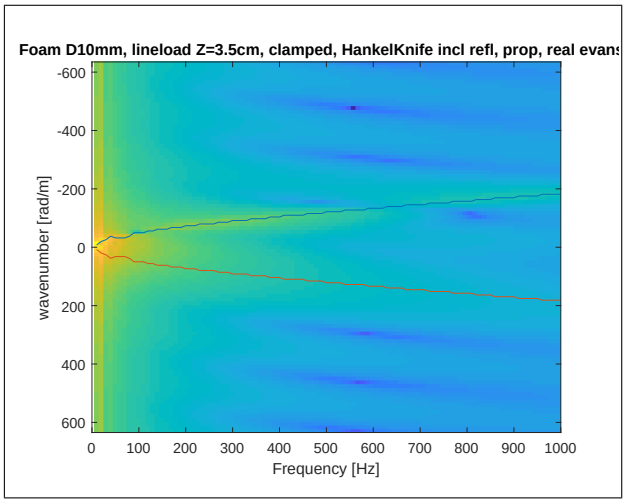

Figure 8. $k-\omega$ spectrum of knife excitated slap (Figure 3), 10mm thick. Color image $k-\omega$ spectrum obtained by means of classical spatial Fourier transform. Solid lines obtained by means of complex wavenumber fit including propagating and evanescent waves, as well as reflected propagating and reflected evanescent waves from the clamped top edge (real part of k shown only).

validity of the wave correlation approach based on Hankel functions, combined with Mindlin's thick plate theory was verified. The approach works well for point excited slabs as well as line excited slabs. In the latter case, the line excitation is approximated by means of an array of in-phase point excitations. The reflection from the edges of the slab is accounted for by means of an image source model. The first order reflections from the edges appeared to be sufficient for the type of slab and frequency range studied.

The optimal wavenumber was search for in 3 dimensions, considering a complex valued propagating wavenumber and a real valued evanescent wave number. Because of this 3D search, this approach requires a large amount of computation time. It appears that the inclusion of evanescent waves are required in order to obtain a better accuracy of the estimated Young's modulus and loss factor.

It was found that at higher frequencies and thicker slabs Kirchhoff's thin shell theory is clearly insufficient. It was also found that for the frequency range and thicknesses studied, Mindlin's plate theory and Lamb wave theory are not very much different (error in wavenumber less than 2% for frequencies up to 1000 Hz and thicknesses up to 10 mm).

From a theoretical point of view it is interesting to see that the Green's functions are the same for Kirchhoff's thin shell theory and for Mindlin's thick shell theory. Thus the wave correlation approach uses the same Green's functions in both cases. However, for the computation of the effective Young's modulus and loss factor of the slab, a choice must be made to use either Kirchhoff's theory or Mindlin's theory.

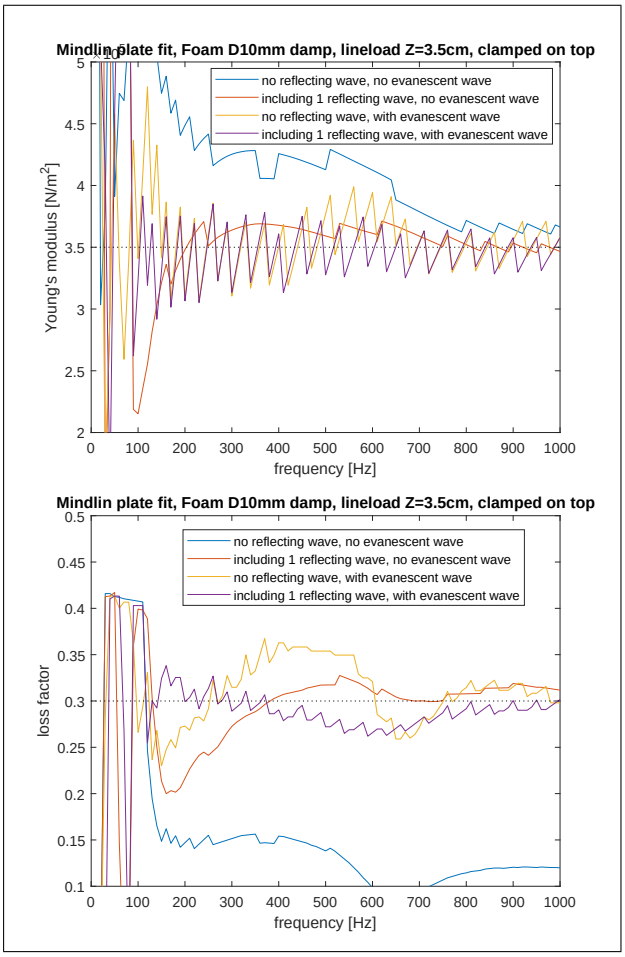

Figure 9. Knife excitated slap (Figure 2), 10mm thick, Young's modulus (top) and loss factor estimate (bottom) based on Mindlin's theory. Blue curve: complex Hankel multiple point source fit without evenscent wave component, Red curve: complex Hankel multiple point source fit with evanescent wave component.

Acknowledgement

This work was supported by a STSM Grant from the COST Action CA15125, "DENORMS". More specifically, this paper is a result of STSM mission of the first author to the university of Ferrara.

References

[1] N.B. Roozen, Q. Leclere, K. Ege, Y. Gerges, Estimation of plate material properties by means of a complex wavenumber fit using Hankel functions and the image source method. Journal of Sound and Vibration 390 (2017) 257-271 http://dx.doi.org/10.1016/j.jsv.2016.11.037

[2] L. R. F. Rose and C. H. Wang, Mindlin plate theory for damage detection: Source solutions, The Journal of the Acoustical Society of America 116, 154 (2004); doi: 10.1121/1.1739482

[3] Karl F. Graff, Wave motion in elastic solids. Courier Corporation, 2012.